INFRARED LASER SCATTERING SYSTEM FOR THE PLASMA DIAGNOSTICS: CO_2 Laser Characteristics

HIRAKI, Naoji
Research Institute for Applied Mechanics, KYUSHU UNIVERSITY

KAWASAKi, Shoji
Research Institute for Applied Mechanics, KYUSHU UNIVERSITY

MURAOKA, Katsunori
Research Institute for Applied Mechanics, KYUSHU UNIVERSITY

https://doi.org/10.5109/7173521

出版情報：Reports of Research Institute for Applied Mechanics. 23 (73), pp.85-96, 1975. 九州大学応用力学研究所
バージョン：
権利関係：

Reports of Research Institute for Applied Mechanics
Vol. XXIII, No. 73, 1975

INFRARED LASER SCATTERING SYSTEM FOR THE PLASMA DIAGNOSTICS

CO_2 Laser Characteristics

By Naoji HIRAKI, Shoji KAWASAKI and Katsunori MURAOKA

As the results of the parametric studies of the double discharge TEA CO_2 laser, the required properties on the laser system for the scattering diagnostics of plasmas are shown to be realized with our CO_2 laser. The direction of the future improvements of the laser performance is also discussed.

1. Introduction

Previously[1], we discussed the possibility of observing the collective scattering of CO_2 laser light from plasmas in terms of the laser power requirements, the necessary optical system, and the detector performance, and showed the feasibility of obtaining the ion temperature of the θ pinch plasma with the present day techniques. Based on this estimate, an oscillator part of a CO_2 laser was constructed and some preliminary results of its operation were described[1]. It is the purpose of this paper to show the details of the CO_2 laser operation.

It is to be noted here that the parameters of the CO_2 laser parts (the discharge length, width, and height, the discharge capacitance and inductance, and the reflectivity of the output window, etc.) have been chosen rather arbitrarily by consulting the results of the published papers. However, the initially intended performance and the direction of the future improvements have been obtained.

Although the emphasis here has, of course, been for the application of the CO_2 laser to the plasma scattering diagnostics, the results might be of value for the laser fusion experiment using CO_2 lasers[2].

2. The double discharge TEA CO_2 laser

There have been various electrode configurations used for exciting the TEA (Transversely Excited Atmospheric) laser. The CO_2 laser we constructed is of the Lamberton and Pearson type with double Rogowski electrodes[3]. The details of the laser and the electric circuit of the system are shown previously[1]. The main dimensions and specifications are summarized in Table 1.

Table 1 Main dimensions and specifications of the TEA CO_2 laser

Discharge length	0.6 *m*
Discharge height	26 *mm*
Discharge width	25 *mm*
Discharge volume	0.39 *l*
Cavity length	1.8 *m*
Radius of curvature of totally reflecting mirror	5 *m*
Reflectivity of plane output window	80 %
Total Inductance of the discharge circuit	400 *nH*
Storage capacitance	0.087 μF

As a system for the collective scattering of laser light from θ pinch plasmas ($n_e \sim 5\times 10^{20}\ m^{-3}$, $T_e \sim T_i \sim 200\ eV$), the CO_2 laser must satisfy the following requirements; i) in order to have a good *S/N* ratio, the output power must exceed 35 *MW*, ii) the divergence of the beam should be within a few *mrad*, iii) the spectral line width of the laser light should not exceed 2~3 *A*, iv) the laser pulse duration should be short enough for a good temporal resolution, and v) the jitter of the delay of the laser output from the discharge trigger should be within a limit, typically of the temporal resolution.

In the following, these requirements are shown to be realized by our CO_2 laser system.

3. The general characteristics of the TEA discharge and lasing

It is by now clear that the mixture of carbon dioxide (CO_2), nitrogen (N_2) and helium (He) is the best available medium for the CO_2 laser output to be extracted from the TEA discharge. In order to find out the optimum mixing ratio and charging voltage of the storage capacitor, the relationship between the discharge condition and the laser output has been studied.

The TEA discharge can be marked by the four distinctly different operating regions. These operating regions are varied by the differences of the electrode configuration, circuit inductance and the storage capacitance. Once these circuit parameters are determined, these operating regions are decided by gas composition, mainly by the He concentration and the ratio of N_2 and CO_2 having a minor effect, and the charging voltage of the capacitor. An example of the divisions of the regions is shown in Fig. 1, in which the charging voltage is taken on the ordinate and the He concentration on the abscissa.

In region (A), the charging voltage is below the breakdown potential for the electrode separation and no discharge occurs. In region (B), a few locarized arcs occur without a uniform glow discharge. The boundary between the regions (A) and (B) is decided by the Paschen condition multiplied by the over-voltage probability (W) defined by Morgan and Morcombe[4]. In region (C), a uniform glow discharge occurs. And in region (D), a few arcs are superimposed on the uniform glow discharge of region (C). There are some indications to suggest that the arc formation is sometime after the initiation of the uniform glow dis-

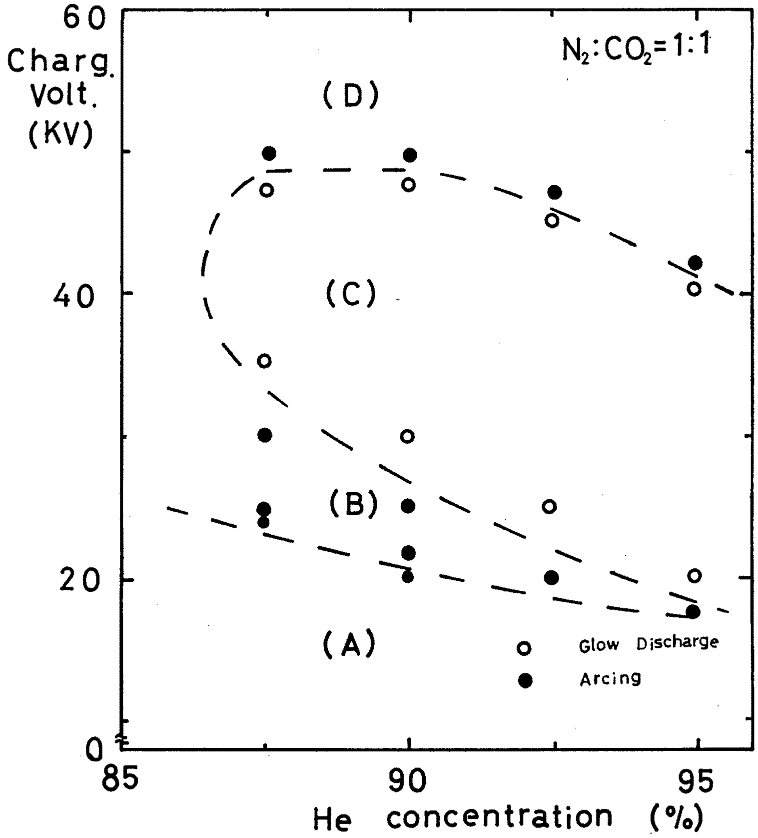

Fig. 1 Operating regions of the TEA discharge.
$N_2 : CO_2 = 1 : 1$.
(A) No discharge, (B) A few localized arcs, (C) glow discharge, and (D) glow discharge superimposed by a few arcs.

charge, but this is not yet settled by the present experiment.

The laser output is obtained in regions (C) and (D), but not in (B). As will be shown in the following sections, the arcs superimposed on the uniform glow discharge have a very deleterious effect on the lasing action and the laser output is abruptly decreased as the operation in region (C) is moved into region (D).

The typical discharge current and the laser output waveforms are shown in Fig. 2, in which (I), (II), and (III) correspond, respectively, to the operations in regions (B), (C), and (D), and the upper trace of each figure shows the current measured by the Rogowski loop and the lower the laser pulse shape measured with the photon drag detector. From these waveforms, the total inductance of the discharge circuit is calculated to be 400 nH, and the plasma resistances

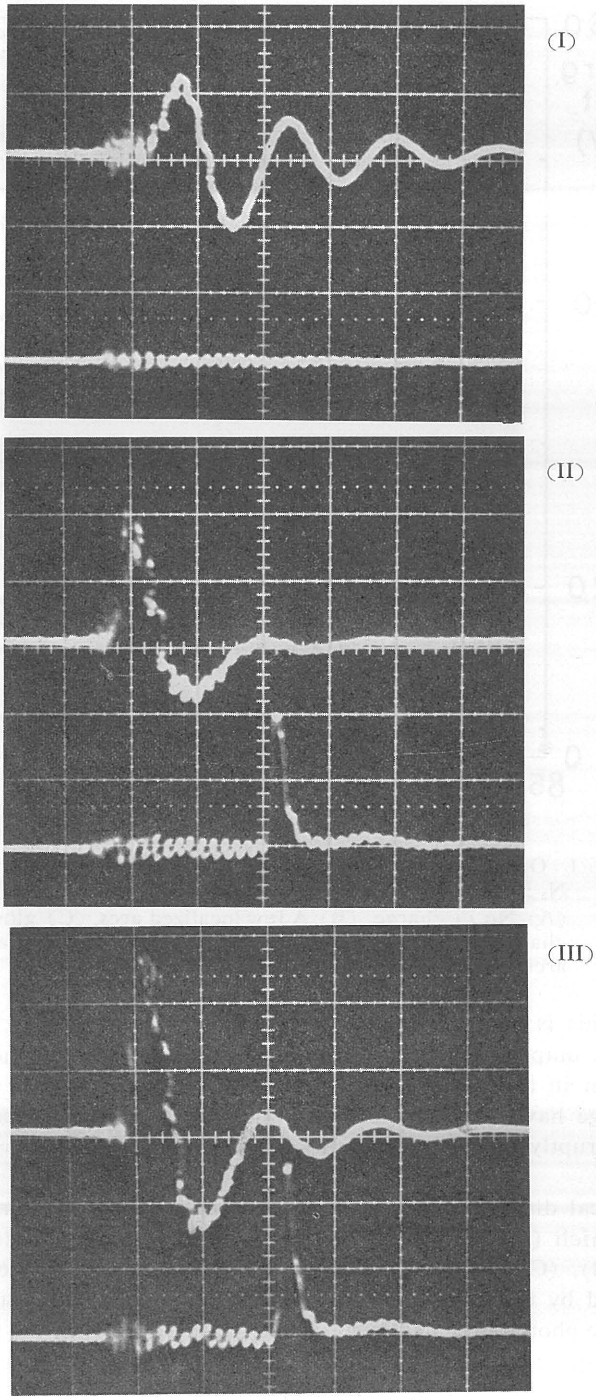
(I)
(II)
(III)

at the discharges are approximately 0.5 Ω for regions (B) and 1.5 Ω for region (C), the latter being consistent with the measurement by Dyer and James[5].

4. The parametric studies of the laser performance

In the previous section, a general behaviour of the discharge and its relationship with the lasing action have been described. In an effort to find out the optimum lasing condition in region (C) of Fig. 1, and to establish the performance of the CO_2 laser, the parametric studies have been carried out.

4. 1. The output pulse energy

The output pulse energy is measured with a dry calorimetre. Figure 3 shows an example of the effect of the volumetric ratio of N_2 and CO_2 on the pulse energy at the fixed relative He concentration. It is clear from this figure that the output energy is not heavily dependent on the ratio of N_2 and CO_2 as long as $(N_2/(N_2+CO_2))$ is between 0.3 and 0.7.

An example of the variation of the pulse energy with the charging voltage

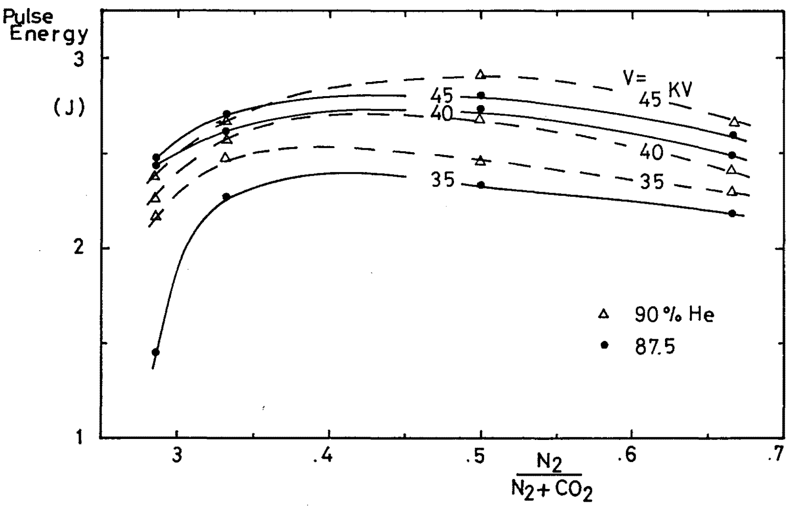

Fig. 3 Variation of pulse energy with the mixing ratio of N_2 and CO_2 at fixed charging voltages and He concentrations.

Fig. 2 Current and laser pulse waveforms at various charging voltages.
He: N_2 : CO_2 = 18 : 1 : 1.
(I) $V_c = 20$ *kV*, (II) $V_c = 40$ *kV*, and (III) $V_c = 50$ *kV*
upper trace: current waveform; vertical scale 5 *kA/div*, time scale 500 *ns/div*,
bottom trace: laser pulse waveform; vertical scale 10 *MW/div*,

for the fixed He concentration and the fixed $N_2 : CO_2$ volumetric ratio is shown in Fig. 4. The abrupt decreases of the laser energy at the high charging voltages show that the discharges there are in region (D) of Fig. 1.

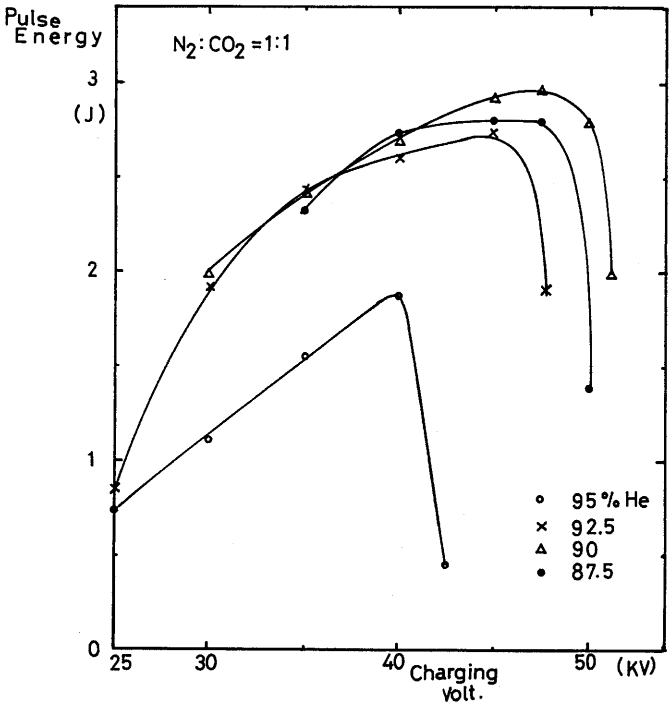

Fig. 4 Variation of pulse energy with charging voltage at fixed He concentrations,
$N_2 : CO_2 = 1 : 1$.

4. 2. The laser pulse shape

The laser pulse shape and the peak power are measured using a photon drag detector with the detective area of 4.5 *mm* ϕ. To avoid the damage of the detective surface, 5 % of the laser power is transmitted with the calibrated polyethelene filter, which is focused on the detector.

Figure 5 shows some examples of the effect of the ratio of N_2 and CO_2 on the pulse shape. The FWHM (full width at half maximum) of the pulses varies from 60 *ns* at $N_2 : CO_2 = 1 : 2.5$ to 120 *ns* at 2: 1.

4. 3. The peak power

Figure 6 shows an example of the effect of the ratio of N_2 and CO_2 on the peak power at the fixed relative He concentration. The highest output power

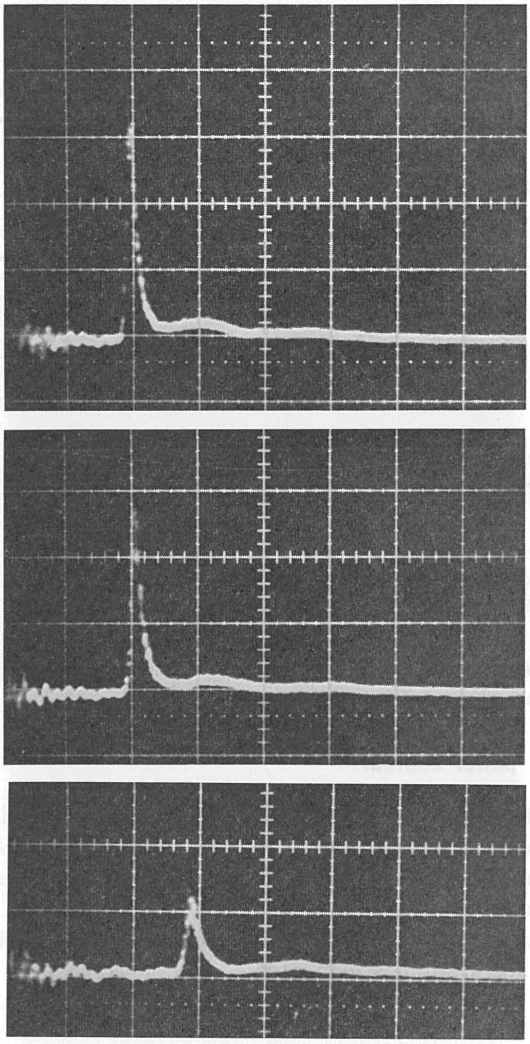

Fig. 5 Fffects of the mixing ratio of N_2 and CO_2 on the laser pulse shape; $V_c = 40$ *kV*, 90 % He;
(A) $N_2 : CO_2 = 1 : 2.5$, (B) $N_2 : CO_2 = 1 : 1$, and (C) $N_2 : CO_2 = 2 : 1$; vertical scale 7 *MW/div*, time scale 500 *ns/div*.

is obtained at $N_2 : CO_2 = 1 : 2.5$, which is explained by the facts that the output energy is rather insensitive to the mixing ratio of N_2 and CO_2 (Fig. 3) and the FWHM of the pulse increases with the N_2 concentration relative to CO_2 (Fig. 5).

Figure 7 shows an example of the variation of the peak power with the charging voltage of the capacitor at the optimum mixing ratio of $N_2 : CO_2 = 1 : 2.5$.

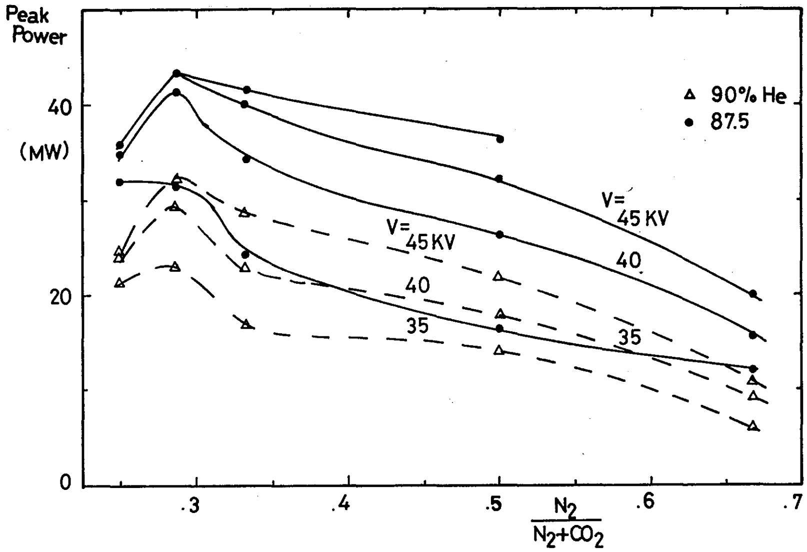

Fig. 6 Variation of peak power with the mixing ratio of N_2 and CO_2 at fixed charging voltages and He concentrations.

The abrupt decreases of the power at the high voltages again correspond to the operations in region (D) of Fig. 1.

4. 4. The iso-peak power contour

Summing up the discharge characteristics and the parametric studies of the laser output, we get a very instructive presentation of results in Fig. 8, in which the iso-peak power contours are shown on the same coordinates as in Fig. 1, for the optimum mixing ratio of N_2: CO_2=1: 2.5. It is seen that the laser power is increased as the charging voltage of the capacitor is increased or the relative He concentration is decreased in region (C).

5. The beam profile and the beam divergence

By a traverse of a photon drag detector with a sensitive area of 2 *mm* ϕ, the beam profiles are measured and the beam divergence is estimated. In Fig. 9, the beam profile thus obtained is shown. In x direction a smoothly decreasing power at both wings is obtained but in y direction side humps exist which contain approximately 25 % of the total power. The origin of these humps is not yet clear, but it could be from the parasitic oscillation at the electrode surfaces. When the laser beam is used for the scattering diagnostics of plasmas, the humps would have to be cut by the divergence limiter.

The beam divergences are, from Fig. 9, 1.8 *mrad* and 3 *mrad* for x and y direction, respectively, which is small enough for the plasma scattering experi-

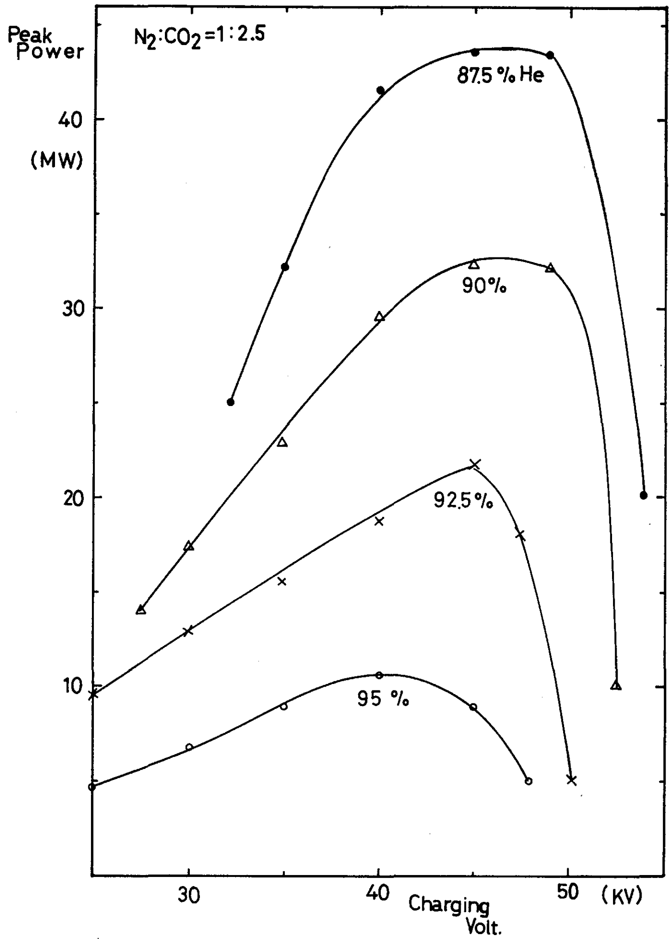

Fig. 7 Variation of peak power with charging voltage at fixed He concentrations;
$N_2 : CO_2 = 1 : 2.5$.

ments.

6. The laser spectral line width

The line spectrum of the laser beam is measured using the spectrum analyzer. The single oscillation at P 20 rotational line is observed. A finer structure is not measured yet, but an experimental report[6] and theoretical estimate show that the line width is about 2∼3 *A* if the single oscillation in a rotational line is realized. The FWHM of the expected scattered light of an example calculation[1] is about 30 *A*, and the line width of 2∼3 *A* is narrow enough for the application.

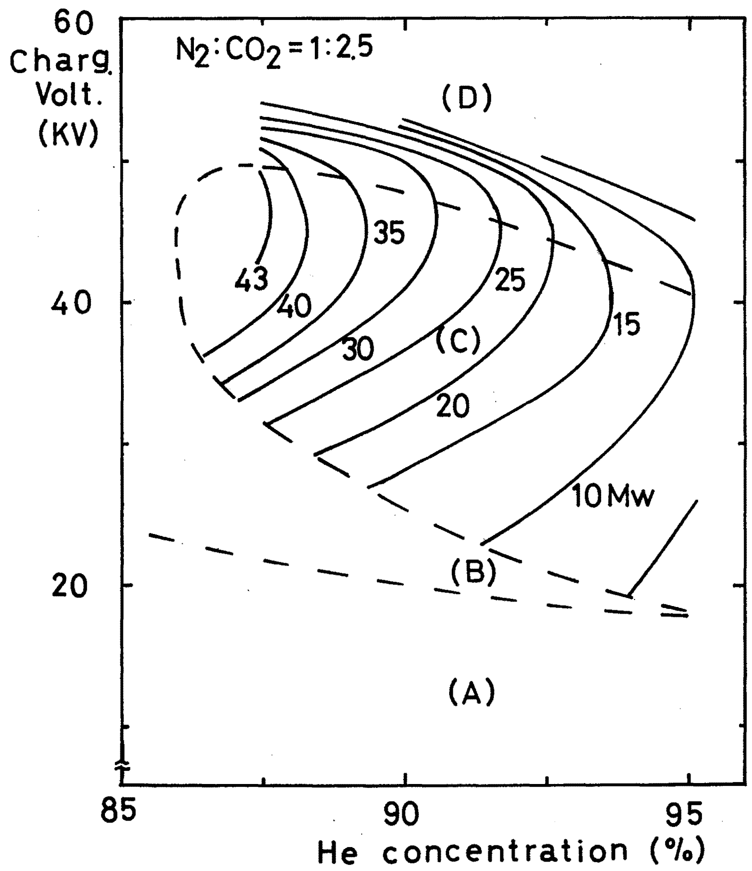

Fig. 8 Iso-peak power contours.

7. The time delay and jitter of the laser output from the discharge trigger

In Fig. 10, the delay of the laser output from the signal input to the pulser for the discharge trigger is shown together with the error bars which are the scatters of the data of ten shots for each point. In applying the CO_2 laser on a plasma scattering experiment, the delay of about 2 μs is of no problem as it could be adjusted by the preset timer, and the jitter of about 150 ns is small enough for the good temporal resolution even for the shortest duration experiment envisaged (1 μs for a turbulent heating experiment).

8. Discussion and conclusion

By the detailed studies of the operation of the double discharge TEA CO_2 laser, i) the discharge condition, ii) the laser output energy, iii) the laser output power, iv) the laser beam profile and divergence, v) the laser spectral line

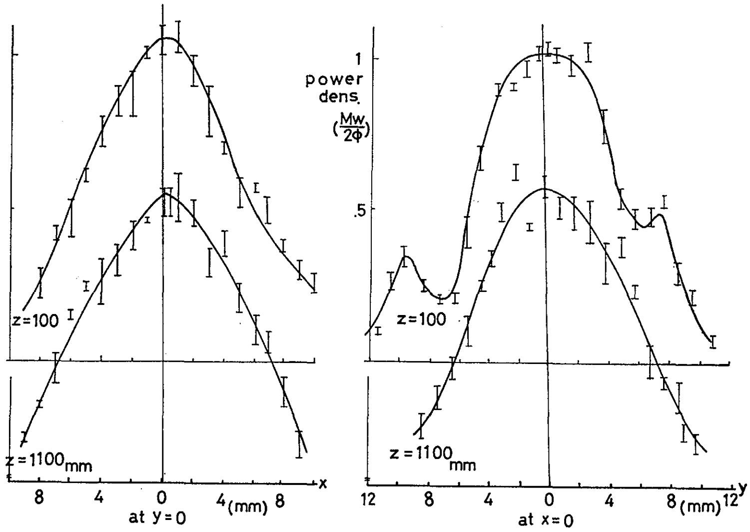

Fig. 9 Laser beam profiles;
x: horizontal direction,
y: vertical direction (the electrodes are at $y=\pm 13$ mm), and
z: distance from the plane output mirror.

width, and vi) the time delay and jitter of the laser output from the discharge trigger, have been established. As long as iv) $\sim$ vi) can be maintained within the allowable limits for the plasma scattering applications, with the variations of discharge parameters, which is the case in the present experiment, the maximum obtainable power (not necessarily the maximum efficiency of converting the input electric energy to the output laser energy) is desirable, as the S/N ratio can be improved from the scattering experiment, or in case the amplification is necessary, the number of the amplification stages can be reduced to achieve a desired output power. In this respect, the presentation of the results in Fig. 8 suggests the direction of the future improvements. Figure 8 shows that at the optimum mixing ratio of N_2: CO_2=1 :2.5 (Fig. 6), and provided that the discharge is in region (C), i) the higher the charging voltage of the capacitor, and ii) the lower the He concentration, the higher the output power. For the present parameters, the contribution from ii) is the more pronounced, and the direction of the future improvements should first be to realize the glow diacharge (C) in lower He concentration. This study is presently being made from the discharge circuit parameter point of view by referring to the various proposals for the arc formation mechanisms[5),7)], and the results will be presented in the near future.

In concluding, we can say that our present CO_2 laser oscillator alone can deliver the desired power with the allowable beam divergence and laser spectral line width for the measurement of ion temperature from the observation of the

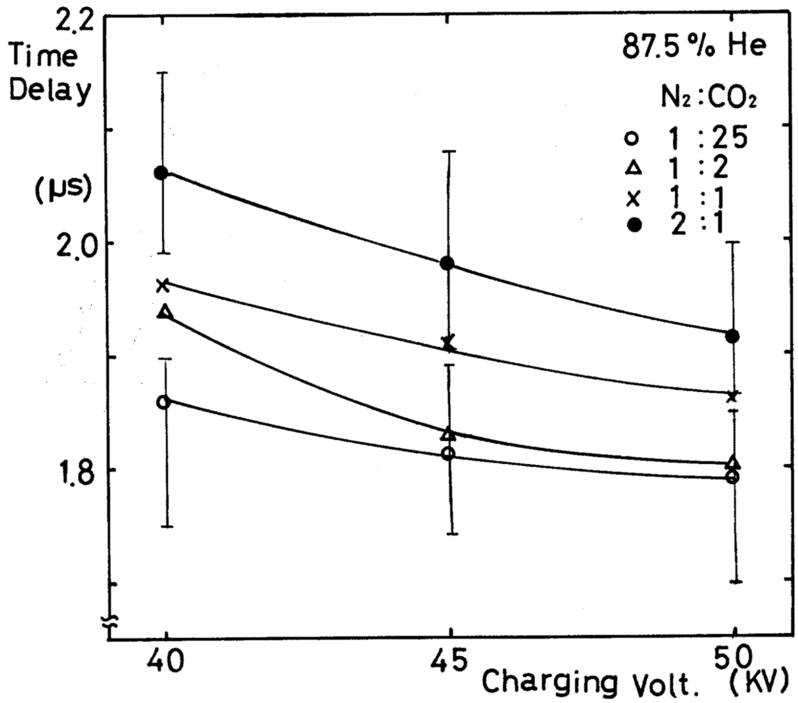

Fig. 10 Variation of delay time of the laser output from the discharge trigger at fixed charging voltages and the mixing ratios of N_2 and CO_2.
The error bars are the scatters of data of ten shots for each point.

collective scattering from θ pinch plasmas. For the turbulent plasma scattering diagnostics, the output power is more than enough and the latter measurement is now being prepared.

References

1) Muraoka, K., Hiraki, N., and Kawasaki, S., Rep. Res. Inst. Appl. Mech., Vol. XXII, No. 70, 1975, p. 177.
2) Crow, J. E., Spalding, I. J., and Wesson, J. A., J. Plasma phys. Vol. 13, Pt 2, 1975, p. 367.
3) Lamberton, H. M. and Pearson, P. R., IEEE J., Vol. QE-8, No. 2, 1972, p. 145.
4) Morgan, C. G. and Morcombe, D., Proc. Phys. Soc., Vol. 66-B, 1953, p. 665.
5) Dyer, P. E. and James, D. J., J. Appl. Phys., Vol. 46, No. 4, 1975, p. 1679.
6) Craig, A. D., Nakai, S., Summers, D. D. R., and Paul, J. W. M., UKAEA Culham Laboratory Report CLM-P 379, 1974.
7) Johns, T. W. and Nation, J. A., Appl. Phys. Lett., Vol. 20, 1972, p. 495.

(Received June 30, 1975)